

The effects of lithospheric thickness and density structure on Earth's stress field

J. B. Naliboff,^{1*} C. Lithgow-Bertelloni,² L. J. Ruff¹ and N. de Koker³

¹Department of Geological Sciences, University of Michigan, MI, USA. E-mail: jbnaliboff@ucdavis.edu

²Department of Earth Sciences, University College London, London, UK

³Bayerisches Geoinstitut, University of Bayreuth, Bayreuth, Germany

Accepted 2011 September 23. Received 2011 September 23; in original form 2010 August 3

SUMMARY

Lithospheric density and thickness variations are important contributors to the state of stress of the plates. The relationship between the lithosphere's isostatic state, subcrustal structure and stress field, however, remains unresolved due to the uncertainties on its thickness, composition and rheology. To study the influence of lithospheric structure on intraplate stresses, we use a new model of global lithospheric structure (TDL) that accounts for the presence of depleted mantle to explore the effects of isostatic compensation, mantle density structure, lithospheric thickness (base depth) and mechanical coupling within the lithosphere on wavelengths >200 km. We compute the mean lithostatic stress (Ω) of $2^\circ \times 2^\circ$ lithospheric columns and then solve for the resulting global 'tectonic' stress field for a homogeneous elastic lithosphere with the finite element package ABAQUS. For a 100 km base depth, a historically common value for lithospheric thickness, tectonic stress patterns are largely insensitive to mantle density structure and match patterns in the world stress map, for both isostatically compensated and non-compensated lithospheric structure. Increasing the base depth up to 250 km to account for thick continental roots, however, leads to sharp variations in the stress field between isostatic lithospheric structure models and TDL as the mantle portion of the lithosphere dominates Ω . Decreasing the model base depths up to 25 km as a proxy for vertical strength variations due to low viscosity channels within the crust or lithosphere as a whole, strongly alters stresses in magnitude, azimuth and regime, as the influence of topography and shallow crustal structure increases. We find that restricting spatial changes in Ω to a specified region to mimic lateral variations in strength also has a large effect on the resulting stresses, which leads us to conclude that regional models may not always be adequate for modelling the stress field. Strong deviations from long-wavelength patterns on the world stress map in models with a shallow ($<<100$ km) or deep ($>>150$ km) uncompensated model base depth likely reflect that the globally averaged lithospheric thickness is close to 100 km and large deviations from this depth generate unrealistic stress patterns related to uncompensated buoyancy forces. Because the stresses are so sensitive to base depth, we conclude that using Ω to represent spatial and vertical variations in lithospheric structure is not an adequate approximation. Our results suggest that future studies must incorporate the full 3-D variations in density and rheology of the lithosphere to elucidate the source and nature of the lithospheric stress field. These studies have become possible with the advent of modern computational tools and advances in our knowledge of lithospheric structure and rheology.

Key words: Composition of the mantle; Dynamics of lithosphere and mantle; Dynamics: gravity and tectonics; Mechanics, theory, and modelling; Rheology: crust and lithosphere; Rheology: mantle.

1 INTRODUCTION

Variations in lithospheric thickness and density produce tectonically significant stresses in the Earth's lithosphere (Artyushkov 1973; Molnar & Tapponier 1978; Dahlen 1981; Fleitout &

*Now at: Department of Geology, University of California, Davis, CA 95616, USA.

Froidevaux 1982; Fleitout & Froidevaux 1983), which can be understood within the framework of lateral variations in the lithosphere's gravitational potential energy (GPE) or the mean lithostatic stress (e.g. Artyushkov 1973; Molnar & Lyon-Caen 1988; Coblenz *et al.* 1994; Ghosh *et al.* 2009).

The basic physics is that lateral variations in lithospheric structure, such as topography, must be supported by horizontal stresses (Jeffreys 1984). Such variations play a particularly significant role in regions with large topographic gradients including mid-ocean ridges, Tibet and Western North America (Molnar & Tapponier 1978; Richardson *et al.* 1978; Dahlen 1981; Turcotte 1983; England & Houseman 1986; England & Houseman 1988; England & Houseman 1989; Richardson & Redding 1991; Richardson 1992; Zoback 1992; Houseman & England 1993; Molnar *et al.* 1993; Jones *et al.* 1996; England & Molnar 1997; Jones *et al.* 1998; Flesch *et al.* 2000, 2001; Liu & Yang 2003; Ghosh *et al.* 2006; Flesch *et al.* 2007; Humphreys & Coblenz 2007; Klein *et al.* 2009).

Lithospheric structure however, involves more than crustal thickness and topographic variations and includes significant lateral changes in both the density and thickness of the mantle lithosphere. The thickness of the lithosphere can vary geographically by hundreds of kilometres (see fig. 1 from Conrad & Lithgow-Bertelloni 2006). In oceanic regions, crustal thickness is nearly constant, but lithospheric thickness depends on the age of the ocean floor and ranges from 0 at the ridge to as much as 100 km for the oldest ocean floor. Estimates of the maximum thickness of the continental thermal lithosphere range anywhere between <200 and >300 km (e.g. Jordan 1975; Rudnick *et al.* 1998; Artemieva & Mooney 2001; Gung *et al.* 2003, Yuan & Romanowicz 2010) and vary strongly as a function of tectonic province.

Variations in density are equally as dramatic, although in comparison to the crustal portion of the lithosphere, fewer constraints exist on the composition of the lithospheric mantle. For the oceans, petrological models for the origin of basalt provide a basis for constructing a model of the lithospheric mantle. An undepleted peridotitic source that partially melts to produce mid-ocean ridge basalt, leaves behind a depleted residue (a harzburgite), the thickness of which depends on the degree of partial melt. As the oceanic lithosphere cools, undepleted mantle becomes part of the lithospheric column and its thickness increases with age. For continents, the picture is less clear and the composition of the continental mantle lithosphere likely varies strongly as a function of tectonic province and age (e.g. Rudnick *et al.* 1998; Artemieva & Mooney 2001; Kaban *et al.* 2003; Artemieva 2006). In the thickest cratonic portions of very fast seismic velocity (e.g. Jordan 1975; Gung *et al.* 2003), the lithospheric mantle may be cold and buoyant (to survive for billions of years), which requires the presence of a depleted layer overlying an undepleted upper mantle layer. This is important for the stress field. For a lithosphere whose base is defined thermally rather than mechanically with no vertical variations in lithospheric strength, the relative density and thickness of the depleted and undepleted lithospheric mantle layers control the mean lithostatic stress and therefore the lithospheric state of stress.

Previous studies have assumed the lithosphere to be a thin sheet of uniform thickness L , over which stresses are computed as depth averaged quantities. The value of L is generally chosen to be some convenient value, for example, $L = 100$ km, which contains the thickest crust. Although this value of L captures much or all of the oceanic lithosphere it misses a significant portion of the continental lithosphere, which can strongly influence GPE (Zoback & Mooney 2003; Pascal 2006). Choosing a uniform lithospheric thickness that captures cratons however, is problematic in tectonically active re-

gions, such as the Western US, where $L < 100$ km (Zandt *et al.* 1995; Li *et al.* 2007; Levander *et al.* 2008). As the density contrast across the base of the lithosphere is small compared with that at the base of the crust, or at the free surface, one might expect computed stresses to be insensitive to the choice of L . However, lateral variations in L are very large and similar to the value of L itself, and this means that the choice of L is of comparable importance to the specification of topography or crustal thickness.

Another common assumption in previous work is that of isostatic equilibrium. However, deviations from isostasy in the lithosphere are substantial and have an important influence on its state of stress (Lithgow-Bertelloni & Guynn 2004; Naliboff 2010). Such deviations may be caused by dynamic topography, which is a determining contribution to Earth's gravitational potential (Hager *et al.* 1985), explains anomalously high topography and bathymetry (Lithgow-Bertelloni & Silver 1998; Conrad *et al.* 2004) and might be crucial for the state of stress in the lithosphere in regions of long-lived subduction (Lithgow-Bertelloni & Guynn 2004). Ascertaining all these components are difficult because it requires information we only have regionally, such as extremely high-resolution images of the lithosphere–asthenosphere boundary (Yuan & Romanowicz 2010), viscosity structure and the degree of mass transfer between upper and lower mantle. A complete examination of the role of dynamic topography or a representation of lateral variations in density at the lithosphere–asthenosphere boundary is therefore beyond the scope of this paper.

An understanding of the deviations from isostasy is essential for a proper formulation of the problem of computing lithospheric stresses. Many previous studies have assumed that stresses in the lithosphere are balanced by lateral variations in the GPE of the lithosphere. However, in the original formulation of the problem, the proper measure of lithospheric weight is the mean lithostatic stress Ω . In the special case of isostatic compensation the two formulations are equivalent. But in the general case the mean lithostatic stress is the proper quantity to examine.

The lithosphere is likely to vary in strength considerably with depth, but the manner in which it does is poorly constrained. The lithosphere may show gradual variations in strength with depth, or may contain weak layers (Kohlstedt *et al.* 1995; Jackson 2002; Burov & Watts 2006; Regenauer-Lieb *et al.* 2006; Burgmann & Dresen 2008; Hartz & Podladchikov 2008; Thatcher & Pollitz 2008). Understanding vertical variations in strength is important because they determine the extent of mechanical coupling between shallow and deep lithospheric regions and the variation of the stress with depth (e.g. Kuszniir & Bott 1977; Bott & Kuszniir 1979; Liu *et al.* 2000; Regenauer-Lieb *et al.* 2006). For example Beaumont *et al.* (2004) have shown that in the Tibet–Himalayan orogeny, which potentially experiences channel flow (e.g. Royden *et al.* 1997; Clark & Royden 2000) there may be multiple mechanical layers that are weakly coupled and exhibit different deformation patterns and rates. In previous global studies of the stress field, vertical variations in lithospheric strength have been examined by varying its thickness, for example, by choosing to include only the strongest, crustal lithosphere, where topographic effects dominate (Klein *et al.* 2009).

Our previous studies have highlighted some of the important remaining uncertainties in our understanding of the global stress field (Lithgow-Bertelloni & Guynn 2004). Although we kept the model base depth constant to 100 km, one end-member model enforced isostatic compensation by varying the density of the lower crust, and the other did not. The patterns of stress so derived (fig. 16 in Lithgow-Bertelloni & Guynn 2004) bore little resemblance to

each other, although the average and maximum stress magnitudes were comparable.

In this study, we take our previous results as the initial point of departure to explore how the lithospheric stress field varies as a function of the density structure of the mantle lithosphere, its average thickness and proxies for vertical and lateral variations in strength. We take advantage of a new model of the global structure of the lithosphere that accounts for the presence of a depleted mantle and whose relevant physical properties (i.e. density) are computed as a function of temperature, pressure and composition in a self-consistent thermodynamic framework.

Our goal is therefore to examine the separate effects of (1) using a more realistic lithospheric thickness and density structure including the depleted mantle lithosphere for the first time, (2) spatial gradients in lithospheric structure, (3) lateral and vertical variations in lithospheric strength and (4) the limitations of assuming a constant depth of the base of the lithosphere, L . We accomplish our goal by examining the sensitivity of the global stress field to the assumption of isostasy, choice of lithospheric model, variations in L and lateral strength.

2 METHODS

We solve for the stress field that balances lateral gradients in the mean lithostatic stress Ω for a homogeneous elastic lithosphere by solving the equations of conservation of mass and momentum in a 3-D spherical shell, for a linearly elastic solid via the finite element method. We compute Ω as

$$\Omega = \frac{g}{L} \int_0^{L+h} dz' \int_0^{z'} \rho(z'') dz'', \quad (1)$$

where g is the gravitational acceleration, L is the thickness of the lithosphere, h the topography and ρ the depth-dependent density. This quantity is the vertical mean lithostatic stress $\Omega = \bar{\sigma}_{zz}$. When computing Ω for each lithospheric column we choose to average by L rather than $L + h$ because our computational shell has uniform thickness.

Our numerical model consists of two vertically and laterally homogeneous spherical layers divided into $2^\circ \times 2^\circ$ equal area 8-node quadrilateral continuum shell elements. Unlike traditional shell elements, continuum shell elements discretize the entire 3-D geometry rather than a reference surface. They are formulated specifically for analyses of stress and displacement and have only displacement degrees of freedom. They are formulated for generalized plane-stress, that is they require that the shear (σ_{zx} and σ_{yz}) components are zero or negligible in the vertical direction, but allow for finite membrane deformation, can include thickness changes and the stresses resulting from it (ABAQUS/Standard 2010). Physically, plane stress implies that lateral gradients in Ω are balanced only by horizontal stress components (σ_{xx} , σ_{yy} , σ_{xy}). Because the lithosphere approximates a thin shell in plane stress, relaxing the plane-stress assumption by using 3-D continuum elements yields nearly identical results (Lithgow-Bertelloni & Guynn 2004). The continuum shell elements adequately capture the flexural response, even though for the wavelengths of the spatial variation in Ω we expect it to be a small contribution to the state of stress. Indeed, our previous study found the bending moments (σ_{zx} and σ_{yz}) to be two orders magnitudes smaller than the normal stresses.

The thickness of the top layer corresponds with the base depth of each model while the lower base layer thickness remains fixed at 100 km. The bottom nodes of the lower layer are pinned in all three

directions and since our model is global no artificial lateral displacement or stress boundary conditions exist. As in our previous work we use the commercial package ABAQUS (ABAQUS/Standard 2010). Following Richardson & Redding (1991), Ω for each lithospheric column is applied to the horizontal faces of a corresponding element in the upper layer of elements, to avoid numerical instabilities related to compression and relaxation of the material.

Following our previous work (Lithgow-Bertelloni & Guynn 2004) we assume an elastic rheology

$$\varepsilon_{ij} = \frac{1+\nu}{E} \sigma_{ij} - \frac{\nu}{E} \sigma_{kk} \delta_{ij}, \quad (2)$$

where ε_{ij} is the strain tensor, σ_{ij} is the stress tensor, ν is the Poisson's ratio and E the Young's modulus. We assign laterally homogeneous elastic properties to both layers of elements with the top layer and bottom layers having, respectively, Young's Modulus values of 10^{11} and 10^6 Pa and a Poisson's ratio of 0.3. The low Young's modulus value of the basal layer prevents transmission of stresses associated with the pinned basal nodes into the upper layer of elements. Since the elastic properties remain constant throughout each layer, their values only influence the calculated strains and not the stress itself.

Our choice of elasticity as a constitutive relation deserves some justification, particularly in view of previous work that assumes the lithosphere is a thin viscous sheet (e.g. England & McKenzie 1982; Flesch *et al.* 2000; Ghosh *et al.* 2006). We feel that elasticity provides a useful end member model with which to understand the stress response of the lithosphere on short time and length-scales. In particular, an elastic constitutive relation permits changes in volume and consequently both isotropic and deviatoric stresses balance lateral gradients in Ω , which are strictly balanced with deviatoric stresses in thin viscous sheet models (*cf.* Appendix). When considering the absolute magnitude of non-lithostatic stresses in the lithosphere, it is important to consider both isotropic and deviatoric stresses as rock strength is related to the difference between the maximum and minimum stress magnitude (i.e. differential stress) and not just the deviatoric stress magnitudes.

2.1 Lithospheric structure

To construct our lithospheric columns we adopt values from Crust 2.0 (Bassin *et al.* 2000) of the density and thickness for ice, sediment and crustal layers as well as topography and bathymetry (Fig. 1a). Layers representing the upper, middle and lower crust are combined into a single layer with an average density (Figs 1c and d). The same is done for unconsolidated and consolidated sediment layers.

To determine the density of continental and oceanic mantle lithosphere we examine two end-member models: an isostatically balanced model and one based on geophysical and petrological constraints (TDL-thermodynamically determined lithosphere). Fig. 2 shows the average density (from the Moho to depth L) for isostatically balanced models (left-hand side) and TDL (right-hand side) for L varying from 100 to 250 km depth.

In the isostatically balanced model, the density of the lithospheric mantle is adjusted so that each lithospheric column is isostatically balanced relative to an Atlantic mid-ocean ridge column (29°N , 43°W) taken from the thermodynamic lithosphere model of de Koker *et al.* (2005). The bathymetric and crustal structure of this reference column is as follows: 3.028 km of water at 1020 kg m^{-3} , 0.07 km of sediment at 1700 kg m^{-3} and 6.5 km of crust at 2861 kg m^{-3} .

In TDL we make use of a new model for Earth's lithospheric thickness and composition (de Koker *et al.* 2005), which

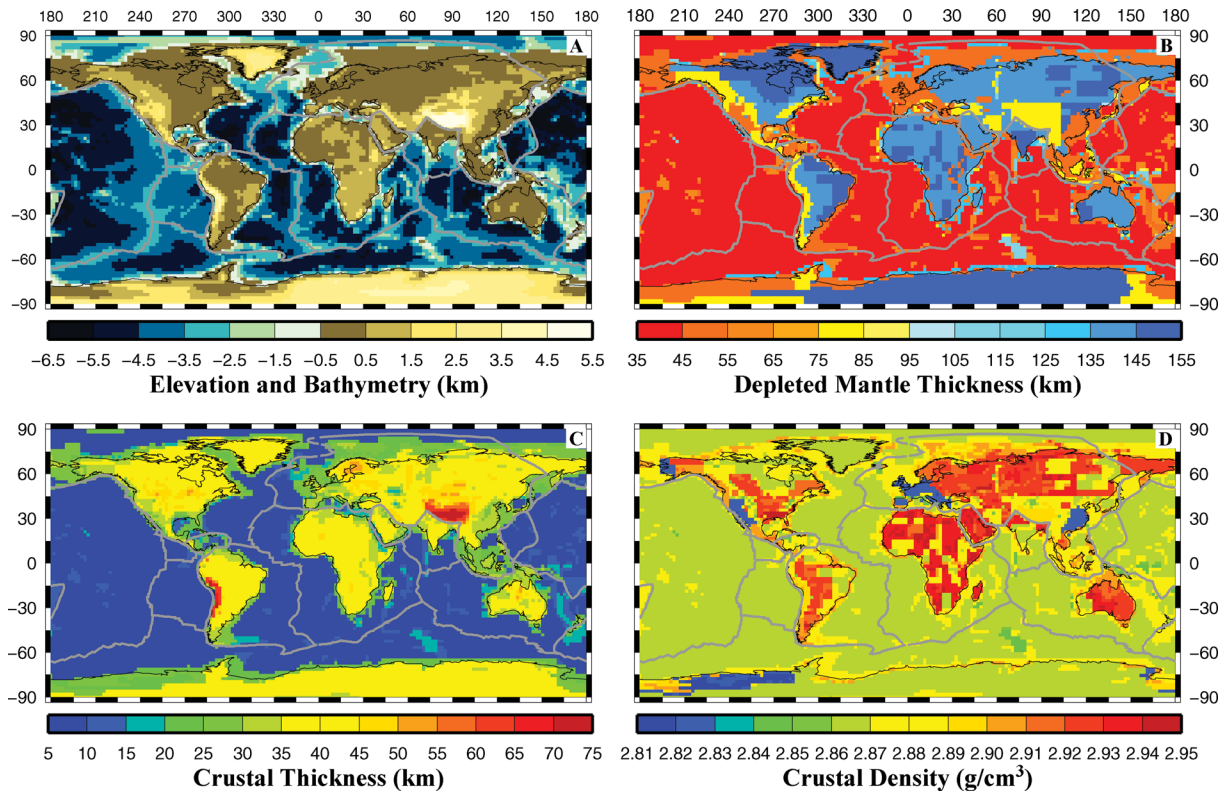


Figure 1. Global lithospheric structure. The crustal data is taken from the Crust 2.0 model, which includes elevation and bathymetry (a) and the thickness and density of ice, sediment and crust (c–d) layers. Displayed crustal thickness and density values are averages of the upper, middle and lower crust layers. The depleted mantle thickness (b) is taken from the TDL model of de Koker *et al.* (2005).

incorporates a layered lithospheric mantle with thermodynamically determined properties. Oceans are regionalized by the age of the ocean floor and continents are divided into four tectonic provinces: cratons, platforms, active margins (including previous orogenies and passive margins). These provinces are obtained by grouping the finer division in CRUST2.0. The lithospheric mantle itself is divided into two layers, (1) the depleted (harzburgite) complement to MORB that originates from partial melting of (2) an underlying enriched pyroclitic source. In oceanic lithosphere, the thickness of the depleted layer is determined by multiplying crustal thickness by a factor (in this case 6.5) proportional to the expected melt fraction needed to produce 6.5 km of MORB crust (Klein & Langmuir 1987; Asimow *et al.* 1995). Because CRUST2.0 does not have variations in the thickness of normal oceanic crust, the depleted layer is assigned a constant thickness of 39 km. The remainder of the oceanic lithospheric mantle is assumed to be pyroclitic. In continental regions the thickness of the depleted layer varies by tectonic province, its thickness obtained by multiplying the thickness of the mafic lower crust as found in CRUST2.0 (Fig. 1d) by a factor, which varies by tectonic province and is roughly proportional to the melt fraction necessary to produce the mafic lower crust. The total thickness of the lithosphere is given by the depth at which the conductive part of the geotherm joins the adiabat ($T_c = 1600$ K), which defines $T(r)$ down to the base of the model.

With the strategy outlined above, de Koker *et al.* (2005) made two important innovations to determine the density of the mantle lithosphere: (1) Compute the density of depleted and undepleted mantle layers as a function of depth using a self-consistent thermodynamic model for mantle petrology and physical properties (Stixrude & Lithgow-Bertelloni 2005), which matches existing petrological and mineral physics experimental constraints; (2) Determine the best

multiplicative factor to obtain depleted mantle thickness, by requiring that the spherically averaged pressure at the base of the model match PREM and its narrow error bounds (Masters & Gubbins 2003).

In TDL the compositions of harzburgite and for pyroclitic are taken from Workman & Hart (2005); oceanic geotherms are computed as a function of age using half-space cooling and the Muller *et al.* (1997) data supplemented as in Xu *et al.* (2006) for regions with no data; continental geotherms (different for each tectonic province) are taken from the literature (Pollack & Chapman 1977; Jaupart & Mareschal 1999; Michaut & Jaupart 2004). The base of the model is chosen at a depth of 350 km below sea level because (1) the depleted layer is not expected to be thicker than this, and (2) there are no major phase transitions close to this depth. The base of the model is therefore assumed to be chemically and lithologically homogeneous. Because isostasy is not enforced in the TDL model, lateral pressure gradients exist at the base of the model, which should reflect the dynamic support of elevation from large-scale mantle flow.

2.2 Lithospheric rheology

We explore the limit of a layer of no strength within the lithosphere at depth S by setting $L = S$. We consider this an end member in which there is full vertical decoupling (i.e. no stress transmission) from layers below depth S . This is akin to separating GPE contributions to the stress field from different parts of the lithosphere (Klein *et al.* 2009). To model lateral variations in strength, we use an end-member proxy, which should capture the extreme case in which a lithospheric region is completely decoupled from surrounding areas. This extreme is unlikely to be present in the Earth, as even

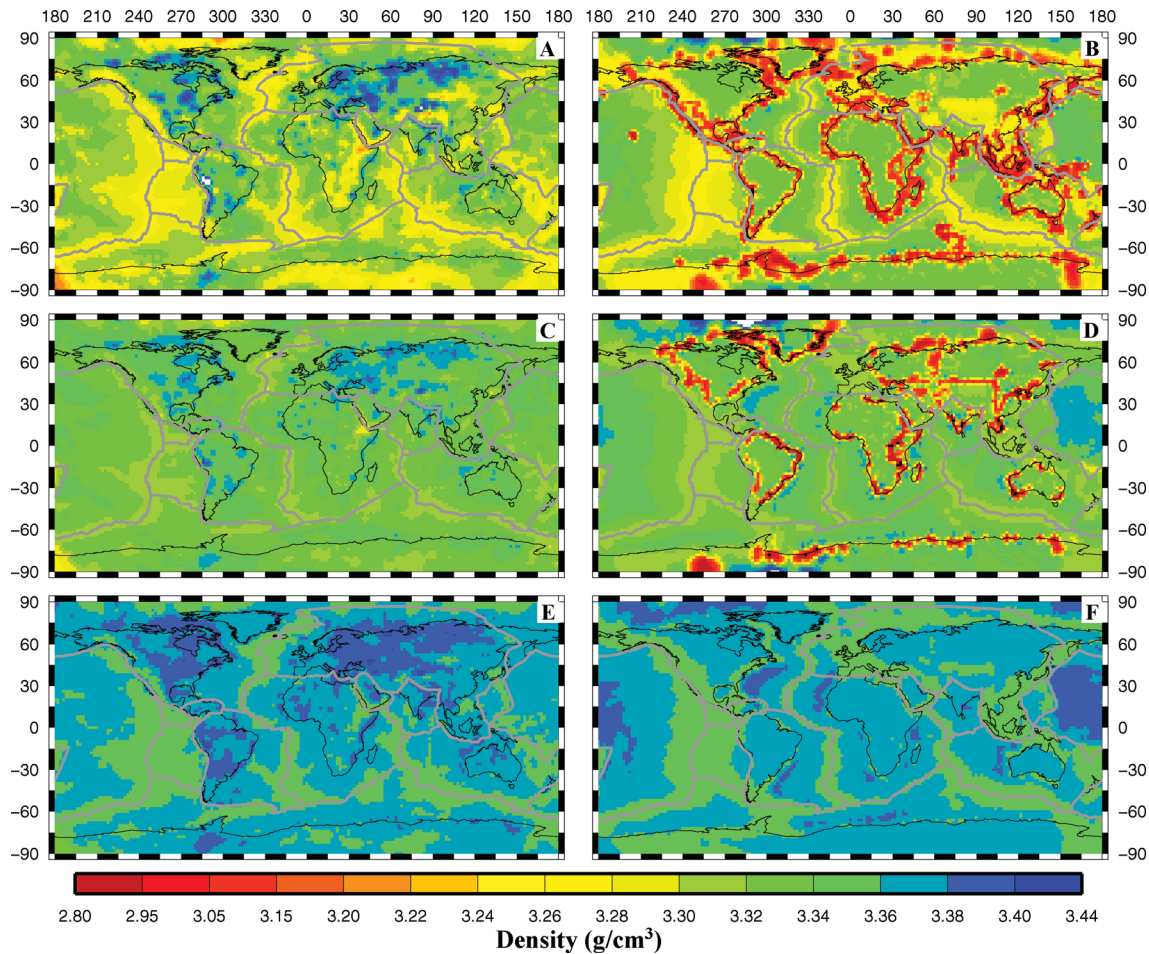


Figure 2. Isostatically adjusted (a–c–e) and TDL (b–d–f) mantle densities for model base depths of 100 (a–b) km, 175 km (c–d) and 250 km (e–f). The density in the isostatically compensated models remains constant throughout the thickness of the mantle portion of each column. The TDL mantle densities are the thickness-weighted average of the depleted and undepleted mantle densities in each column.

across rheological boundaries a portion of the stress normal to the boundary will be transmitted. Besides allowing a crude first-order examination of lateral variations in strength, it also yields a baseline with which to assess differences between global and regional analyses. In selected models, we modify the lithospheric structure of each column outside the region of interest and set it equal to the lithospheric structure of the reference oceanic column used for isostatic adjustments. This removes the source of stress outside the region of interest, although the model is still global and no lateral displacement boundary conditions are imposed.

3 RESULTS

3.1 Reference models

We start with two models containing a commonly assumed 100 km base depth and either an isostatically adjusted (Fig. 3a) or thermodynamically determined (Fig. 3b) mantle density. The mean lithostatic stress and resulting tectonic stress patterns in these models are designed to serve as a reference point for the proceeding models with different base depths or lateral stress boundary conditions. Although notable differences exist between the average density of the isostatically compensated (Fig. 2a) and TDL mantle structures (Fig. 2b), especially near continental margins, the mean lithostatic stress distribution and resulting tectonic stress patterns are quite

similar. This in part reflects the strong influence of topography and crustal density for a 100 km base depth, which limits the influence of mantle density variations. However, enforcing isostasy minimizes gradients in Ω and consequently slightly lowers tectonic stress magnitudes in many regions compared to the TDL mantle density model. The largest deviations in the tectonic stress patterns between the two models occur in the polar regions and near continental margins where the largest density variations also exist (Figs 2a and b).

The tectonic stress patterns in general strongly resemble previously published stress models for a 100 km base depth (Steinberger *et al.* 2001; Lithgow-Bertelloni & Guynn 2004; Ghosh *et al.* 2009) and contain many of the long-wavelength patterns observed in the world stress map (Zoback 1992). Tectonic stress magnitudes (Fig. 3) range from <10 MPa to tens of megapascals, with the largest tectonic stress magnitudes occurring in regions with large topographic gradients (e.g. pacific margin of North and South America, Tibet and Eastern Africa). The maximum tectonic stress magnitudes reach 75 MPa in Tibet for the TDL mantle structure (Fig. 3b).

3.2 Deep lithospheric structure

Moving the model base to greater depths increases the lithospheric thickness and places the centre of gravity lower in the lithospheric column, thereby reducing the influence of topographic gradients on

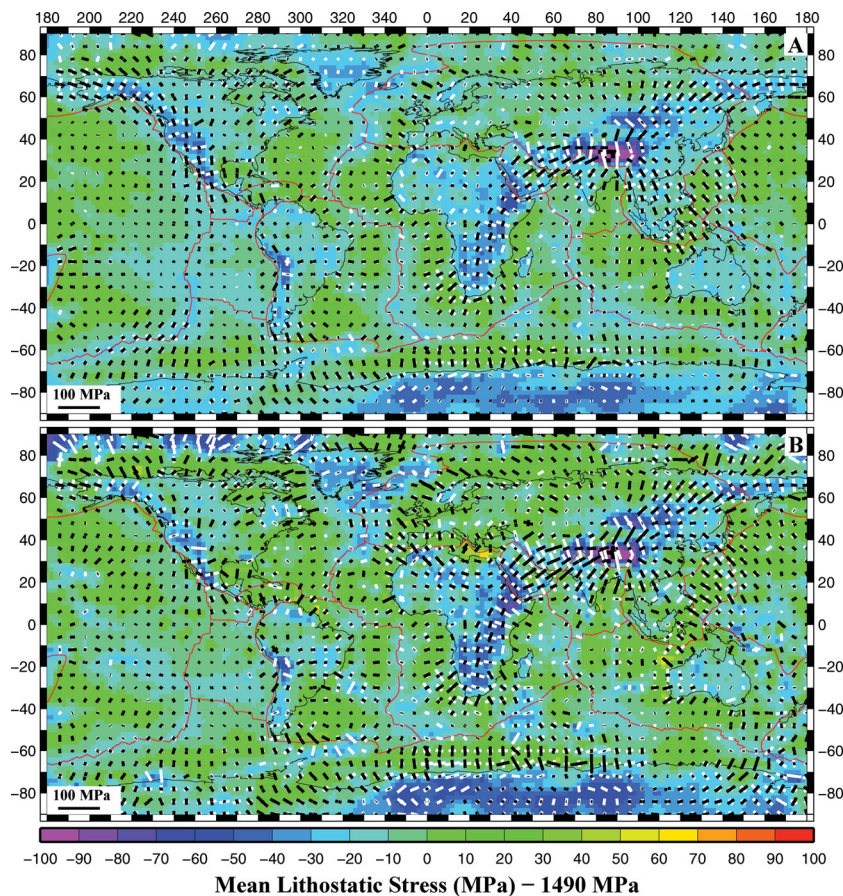


Figure 3. Variations in global mean lithostatic stress (Ω) and the tectonic principal stresses balancing these variations for a 100 km base depth. Regions with large negative values of Ω often correspond with topographically high regions and are characterized by extensional principal stresses (white bars, compression \sim black bars). Mean lithostatic stress and tectonic stress patterns are shown for models with isostatically adjusted (a) and TDL (b) mantle density structures. The globally averaged mean lithostatic stress values are (a) 1500 MPa and (b) 1496 MPa. To compare mean lithostatic stress values in (a) and (b) directly, a reference mean lithostatic stress value was removed from each field prior to plotting rather than subtracting the globally averaged values. The reference value was taken from a lithospheric column in the isostatically adjusted model corresponding geographically to the isostatic reference column in the TDL model.

tectonic stress patterns. For the case of the isostatically adjusted mantle structure with a 175 km base depth (Fig. 4a), global tectonic stress patterns are similar to those for the 100 km base depth model. The similarity of the patterns reflects that the mean lithostatic stress variations remain strictly related to surface and Moho topography, while the deeper base depth reduces the lateral variations in mantle density required to enforce isostasy (Fig. 2). Increasing the base depth reduces lateral variations in Ω thereby reducing stress magnitudes, in both continents and oceans by roughly the same amount. Increasing the base depth to 250 km (Fig. 5a) largely reproduces these trends.

In TDL, increasing the base depth incorporates in the lithospheric column additional mantle density variations that have no assigned role in enforcing isostatic balance. As a result, the additional mantle in each column may drive the models towards or away from regional isostatic compensation, and increase or decrease regional mean lithostatic stress gradients. The mantle incorporated by increasing the base depth from 100 to 175 km leads to larger gradients in the mean lithostatic stress distribution (Fig. 4b), particularly across tectonic provinces where different mantle geotherms influence the density structure. Increasing L from 100 to 175 km magnifies the tectonic stress magnitudes regionally while the orientations remain similar (i.e. Antarctica, Mediterranean, Ural Mountains, Western Australia) while in other regions the stress orientation is

strongly modified as well (i.e. Western North America and Andes). Increasing the base depth to 250 km (Fig. 5b) generates the largest Ω gradients and resulting tectonic stress magnitudes despite the lowest averaged mantle density variations (Fig. 2f), where the tectonic stress field in many regions strongly deviates from the 100 km reference model and long-wavelength patterns in the world stress map. In many regions, the tectonic stress magnitudes are more than a factor of 2 larger than those in the isostatically compensated model with a 250 km base depth (Fig. 5).

3.3 Effects of strength variations within the lithosphere

Decreasing the base depth from 100 to 50 km for the TDL mantle density structure (Fig. 6) illustrates the development of large-scale stress patterns related to regions of high topography. As the base depth decreases the relative contribution of topography to the mean lithostatic stress increases, as shown in Tibet, the Western US and the Andes. The larger influence of the topographically highest regions for $L = 50$ km reveals a long-wavelength stress pattern where compressional stresses run parallel to a large percentage of the Pacific Plate boundary (Fig. 6b) and increase in magnitudes by up to a factor of 2.

To examine possible lateral variations in strength, we limit the sources of stress to the regional scale (Fig. 7). Stress fields are

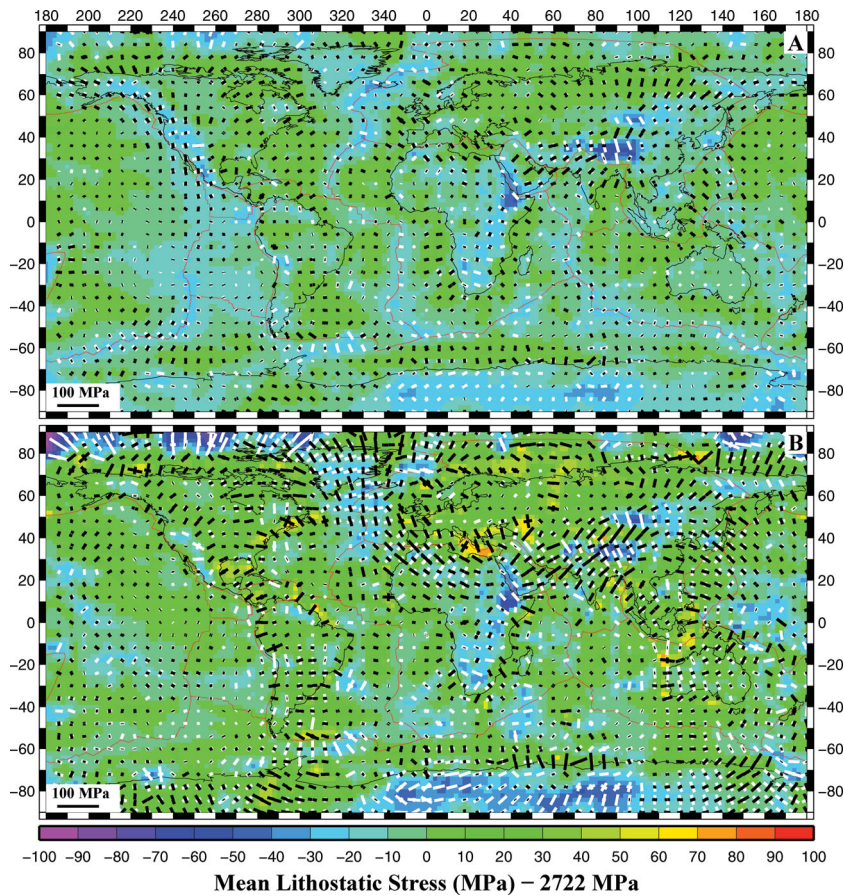


Figure 4. Mean lithostatic stress variations and resulting tectonic principal stresses for a 175 km model base depth and isostatically adjusted (a) or TDL (b) mantle density structures. The globally averaged mean lithostatic stress values are (a) 2727 MPa and (b) 2719 MPa. The subtracted reference value was determined as in Fig. 3.

localized by removing spatial gradients in Ω outside the region of interest. The comparison shows that variations in Ω can have a significant influence on the stress field even if they occur far outside the region of interest. For example, for the model with $L = 100$ km and TDL mantle structure (Figs 3b and 7a) the stress regime in western North America becomes more extensional by assigning a constant Ω value outside the North American continent (Fig. 7b). The azimuth of extensional stresses in Western North America oriented perpendicular to the plate boundary remain largely unaffected by the stress boundary conditions, although in Alaska and the Western Continental US a component of plate-boundary perpendicular extension is translated into plate boundary parallel extension. Extensional stress magnitudes in Greenland and the North Atlantic increase due to a decrease in mean lithostatic stress to the East. Restricting the mean lithostatic stress variations further to within the Continental US and neighbouring Atlantic (Fig. 7c) reduces extensional tectonic stress magnitudes in the Western US, which decrease significantly due to the smaller Ω variations across neighbouring Western Pacific regions. Extensional tectonic stress magnitudes along the mid-Atlantic ridge also decrease due to the reduced local mean lithostatic stress variations.

Maintaining the regional stress model and decreasing L from 100 km (Figs 8a and 9a) to 50 km (Figs 8b and 9b) and 25 km (Figs 8c and 9c) increases extensional tectonic stress magnitudes in the topographically high Western US as lithostatic stress related to topography is averaged over a thinner column. For $L = 100$ km, the extensional tectonic stress magnitudes in the Western US range

on average between 5–15 MPa, which for a 50 km and 25 km base depth increase, respectively, to 10–20 MPa and 15–25 MPa.

Compressional and extensional tectonic stress magnitudes in the continental interior (Fig. 8) increase by 50–100 per cent as the base depth decreases by a factor 2, which is a response to both E–W and N–S larger mean lithostatic stress gradients. At base depths of 50 km and 25 km a strike-slip state of stress dominates the majority of the continental USA interior and Western Atlantic basin, which contrasts sharply with the 100 km base depth stress patterns and observed regional stress patterns (Zoback 1992). Notably, for a 100 km base depth the tectonic extensional stress magnitude range of 5–15 MPa in the Western USA is very close to the deviatoric extensional stress magnitude ranges of 5–10 MPa (Flesch *et al.* 2007; Humphreys & Coblenz 2007) reported in previous regional modelling studies for a 100 km base depth.

4 DISCUSSION

4.1 Sources of tectonic stress

To understand the magnitude and pattern of our stress results we can make use of an approximate 2-D theory that also assumes plane-stress (Appendix). Our previous numerical results based on the full 3-D equations, show that the approximations made in the 2-D theory are not severe (Lithgow-Bertelloni & Guynn 2004). For example, shear stresses acting on the vertical face are two orders of magnitude smaller than other components, a key approximation in

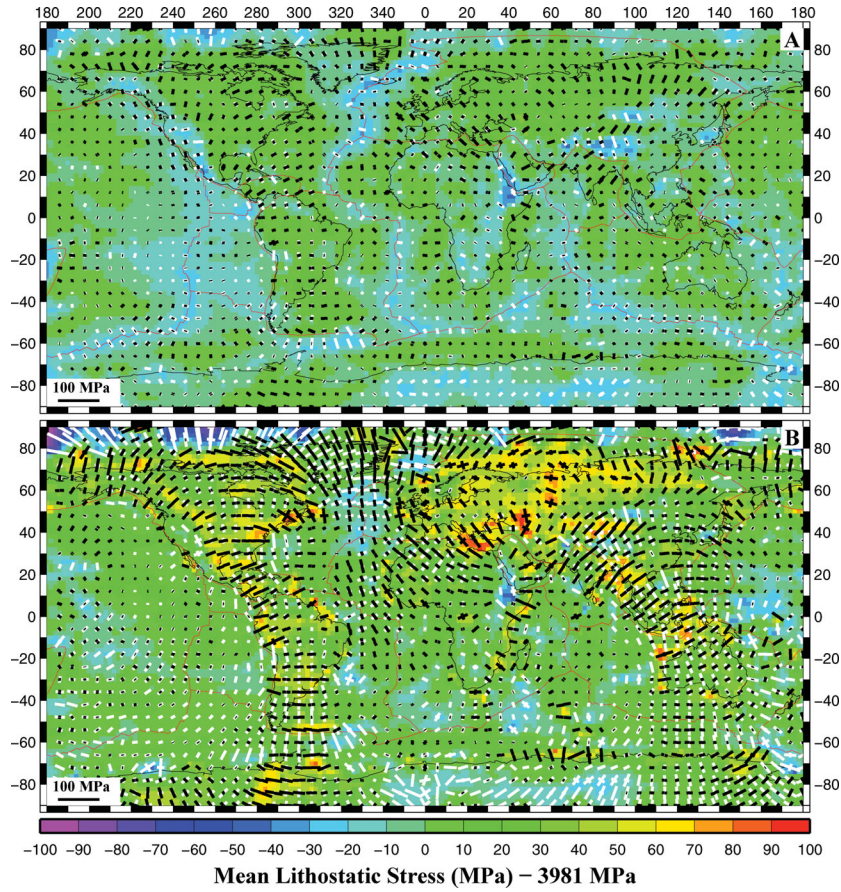


Figure 5. Mean lithostatic stress variations and resulting tectonic principal stresses for a 250 km model base depth and isostatically adjusted (a) or TDL (b) mantle density structures. The globally averaged mean lithostatic stress values are (a) 3983 MPa and (b) 3965 MPa. The subtracted reference value was determined as in Fig. 3.

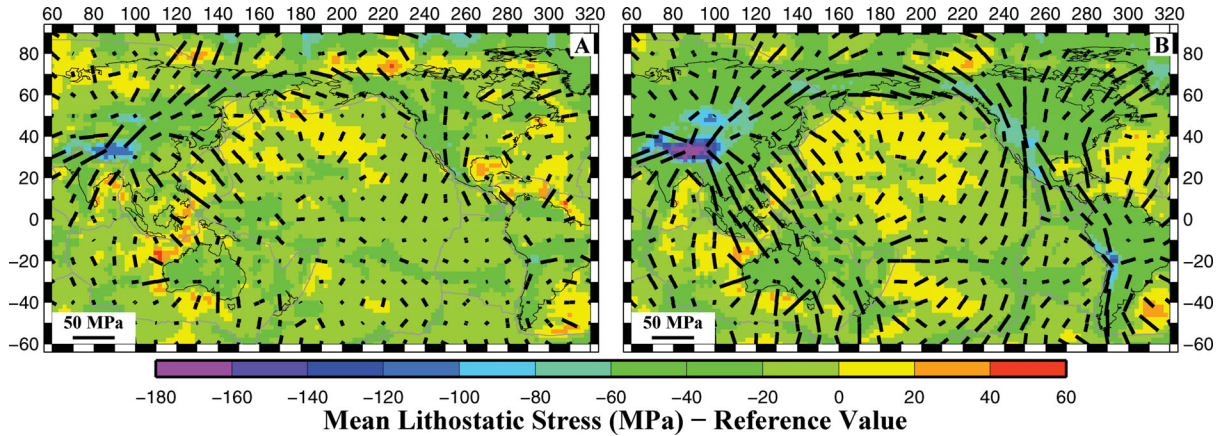


Figure 6. Mean lithostatic stress variations and resulting compressional tectonic principal stresses for a TDL mantle density structure and a 100 km (a) or 50 km (b) model base depth. The reference values subtracted from the mean lithostatic stresses are 1482 MPa (a) and 678 MPa (b), which represent the mean lithostatic stress of the isostatic reference column for base depths of 100 and 50 km.

the theory. The advantage of examining the 2-D theory is that the problem can be expressed in a way that offers considerable physical insight.

The key result of the 2-D theory derived in Appendix is that lateral variation in Ω are supported by lateral variations in the depth-averaged tectonic stress $\bar{\sigma}_{ij}^T$

$$\frac{\partial \bar{\sigma}_{ij}^T}{\partial x_j} = -\frac{\partial \sigma}{\partial x_i} i, \quad j = x, y, \quad (3)$$

where $\sigma_{ij}^T = \sigma_{ij} - \sigma_{zz} \delta_{ij}$, σ_{ij} is the stress tensor, σ_{zz} is the lithostatic stress (sometimes called the lithostatic pressure), i and j run only over x and y , and we neglect shear stresses (σ_{xz} , σ_{yz}) acting on the vertical faces. In general, the tectonic stress tensor is not identical to the deviatoric stress tensor that arises naturally in the development of fluid dynamics as the difference between the stress and the pressure (*cf.* Appendix). The two are related by

$$\sigma_{ij}^T = \tau_{ij} - \tau_{zz} \delta_{ij} \quad (4)$$

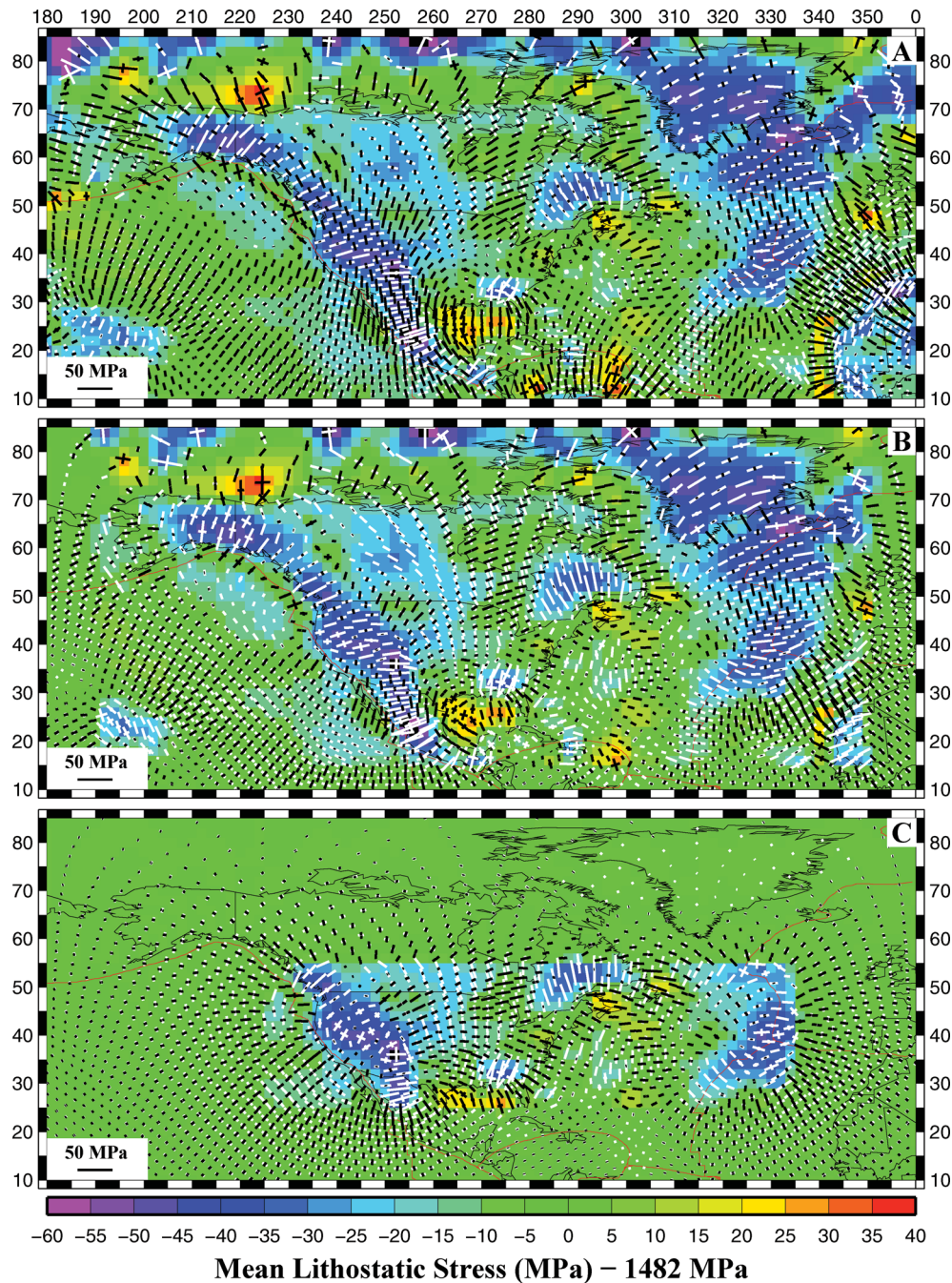


Figure 7. Global (a), plate (b) or regional (c) mean lithostatic stress variations and resulting tectonic principal stresses for a 100 km model base depth and TDL mantle density structure. The global model (a) is the same as Fig. 3(b). Mean lithostatic stress values are assigned the same value as the reference column outside of (15°N – 85°N – 170°W – 10°W) for the plate model (b) and (25°N – 55°N – 135°W – 25°W) for the regional model.

via the definition of deviatoric stress

$$\sigma_{ij} = \tau_{ij} + \frac{1}{3}\sigma_{kk}\delta_{ij} = \tau_{ij} - p\delta_{ij} \quad (5)$$

and the difference between the lithostatic stress and pressure

$$\tau_{zz} = \sigma_{zz} - \frac{1}{3}\sigma_{kk} = \sigma_{zz} + p, \quad (6)$$

which vanishes for an isotropic stress state, such as one may find in a stationary fluid. The tectonic stress (σ_{ij}^T) is a generalization of the term tectonic pressure introduced by Mancktelow (2008); the tectonic pressure is $1/3\sigma_{kk}^T$. Substituting eq. (4) into eq. (3) recovers

the result of England & McKenzie (1983), who frame their results in terms of the deviatoric stress.

We consider the tectonic stress to be a more complete measure of the forces that control the response of the lithosphere to the lateral variations in structure that arise in the course of geological history. Because the lithosphere is not a pure static fluid, the pressure is not simply related to the lithostatic stress due to the weight of the overlying column of rock (Appendix). Rather, it is the spatial gradients in the vertical component of the stress tensor (σ_{zz}) and the shear stresses acting on the vertical face (σ_{xz} , σ_{yz}) that balance the weight of the overburden as required by the equation of mechanical

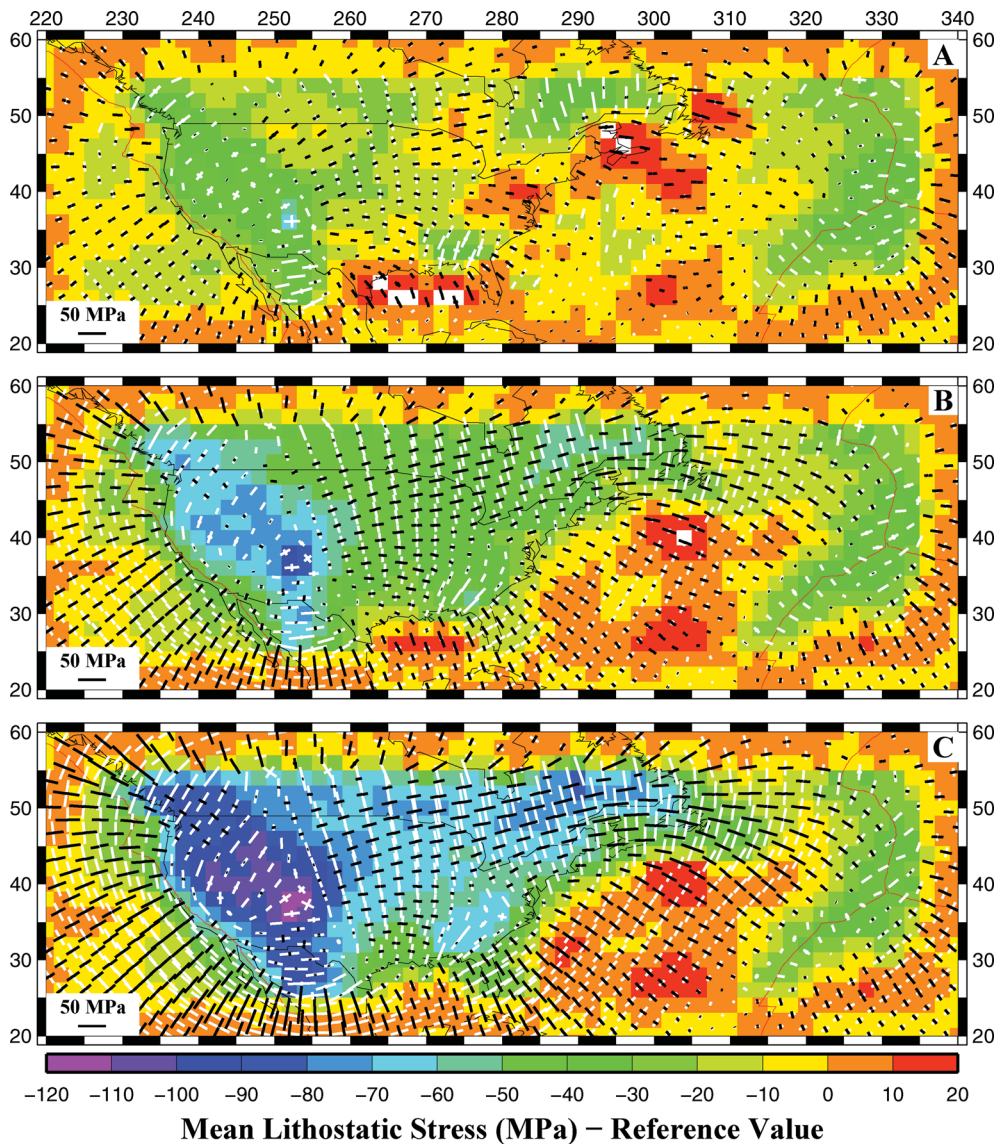


Figure 8. Mean lithostatic stress and resulting tectonic principal stresses for a TDL mantle density structure, regional stress boundary conditions (25°N – 55°N – 135°W – 25°W) and 100 km (a), 50 km (b) and 25 km (c) model base depths. Average mean lithostatic stress values are subtracted as in Fig. 6, (a) 1482 MPa (b) 678 MPa and (c) 286 MPa. (a) is identical to Fig. 7(c), but colour scales have been changed to capture the full range of stress magnitudes.

equilibrium (eq. A2). In our previous work we inaccurately referred to the tectonic stresses as deviatoric (Lithgow-Bertelloni & Guynn 2004).

The simple relationship between $\bar{\sigma}_{ij}^T$ and Ω embodied in eq. (3) allows us to interpret our numerical results. For example as Ω decreases on a N–S transect from Siberia into Tibet the tectonic stress becomes more extensional (positive) (Fig. 3). In regions of high topography, like Tibet or western North America, we expect the magnitude of σ_{ij}^T to exceed τ_{ij} : in these regions of large negative values of Ω , $\tau_{zz} < 0$ and $\tau_{ij} > 0$ (extensional) so that σ_{ij}^T is more positive yet, that is $\sigma_{ij}^T > \tau_{ij}$.

4.2 Deviations from isostasy

Deviations from isostasy are expected because some fraction of the Earth’s topography is dynamically supported by mantle flow. For example, the southern African craton where crustal thickness

is no more than 40 km, but elevations exceed 1500 m is likely supported by the dynamic topography from a large-scale upwelling in the mantle (Lithgow-Bertelloni & Silver 1998). The effects of dynamic topography are evident in the isostatic model (Fig. 2): the mantle under Africa is lighter than the reference column and in regions of long-lived subduction, such as under North America and Eurasia, the mantle is heavier. Our TDL model of lithospheric structure instead implicitly includes dynamic topography by using the observed topography and geophysically constrained lithospheric structure and not enforcing isostatic compensation. Therefore dynamic topography is a major contributor to Ω (Lithgow-Bertelloni & Guynn 2004; Ghosh *et al.* 2009). As a result the values of Ω in southern Africa and other regions of large dynamic topography are much more negative than in the isostatically compensated model (Fig. 3) and resulting stress magnitudes are greater.

To isolate the effects of dynamic topography on the stresses it is not enough to enforce isostatic compensation, particularly in the

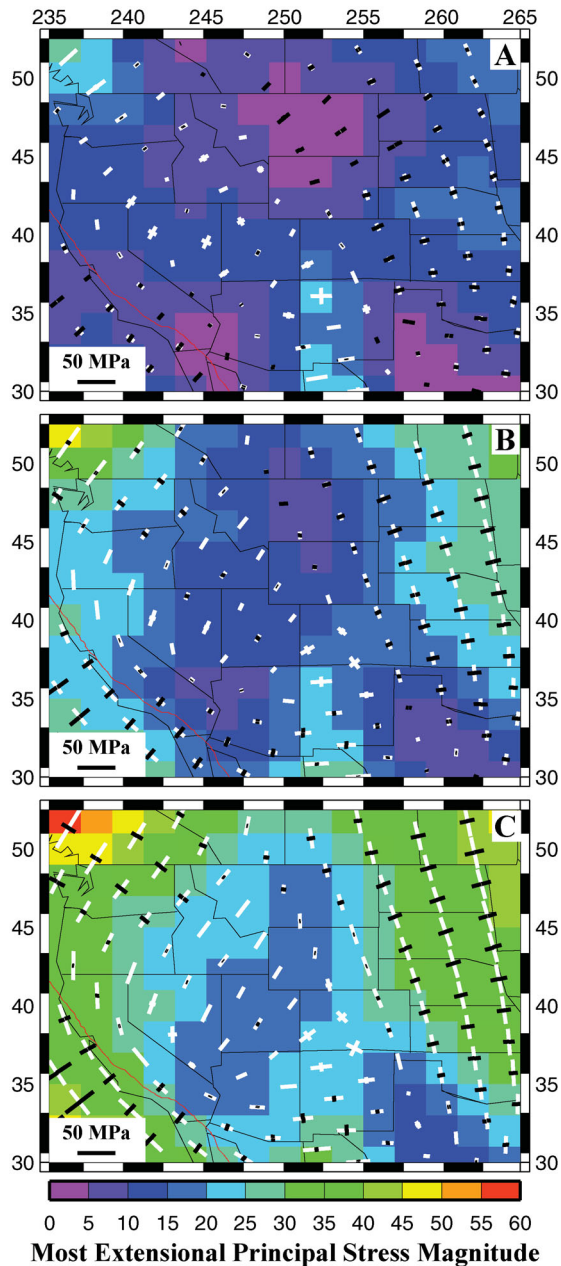


Figure 9. Western US tectonic principal stresses and most extensional tectonic principal stress magnitude for a TDL mantle density structure, regional stress boundary conditions (25°N – 55°N – 135°W – 25°W) and 100 km (a), 50 km (b) and 25 km (c) model base depths.

context of a constant base depth. At a constant L , adjusting the density or elevation of a lithospheric column will mix together density and thickness changes in the mantle portion of the lithosphere and dynamic topography due to mantle flow. Instead, the dynamic component of topography must be removed before, either by using mantle flow models that match relevant global geophysical observables (e.g. geoid and plate motions) or by accounting for the isostatic component of topography due to lithospheric structure. However, both of those approaches may have large errors, because the amplitude of dynamic topography and global lithospheric structure are uncertain. This is important, because the effects of dynamic topography on stresses are large (Lithgow-Bertelloni & Guynn 2004) and

unavoidable even in the presence of a globally weak asthenosphere (Naliboff 2010).

4.3 Variations in L

Away from regions of long-lived subduction and large mantle upwellings we expect the dynamic support to be minimal and for topography to be isostatically compensated. Regions of high topography and thin crust (e.g. western North America) have been explained by the presence of lighter (hotter) mantle. The density of the mantle required to balance the topography is undetermined and trades off with the assumed thickness of the mantle column. For example, the isostatic models in Figs 3–5 all assume the same isostatically compensated topography. However, the stress magnitudes and to a lesser extent pattern, does depend strongly on the assumed level L . As L deepens, gradients in Ω decrease as more mantle is included in the lithospheric column, so that the magnitude of balancing tectonic stresses decreases and stress patterns become more uniform.

In TDL as L deepens there is no systematic decrease in stress magnitudes and the pattern changes significantly. The reason is that model TDL, unlike the isostatically compensated model, contains deep laterally varying lithospheric structure to the depths of the thickest lithosphere (~ 250 km). The role of lateral variations in the mantle lithosphere, including the presence of depleted mantle, has not been previously addressed in studies of the stress field. For example, the signal of Tibet is muted (Figs 3–5) by the presence of relatively light underlying mantle as L is increased beyond a 100 km.

The importance of lithospheric mantle density highlights the importance of the choice of base level L , which should be deep enough to capture deep lithospheric structure. On the other hand, by choosing a uniform deep value of L we also capture substantial amounts of asthenosphere. To avoid capturing asthenosphere we might choose a shallower value of L , but this would neglect deeper sources of stress arising from mantle lithospheric structure deeper than L .

To gain insight into the significance of the base level L we may compare it with the historical concept of depth of compensation. The depth of compensation is the depth below which the stress is isotropic and homogeneous in a static fluid. In the classic problem of isostasy the depth of compensation may be chosen as any depth within the fluid layer, that is, below the lithosphere. In the Ω formulation, L represents a particular choice of the depth of compensation that is coincident with the base of the strong layer. The formulation does not capture radial variations in lithospheric strength or allow lateral variations in the depth of the base of the lithosphere. These limitations are particularly evident in the muting of signals in the isostatic models and in the large variations in stress patterns in TDL with variations in L (Figs 4 and 5). In TDL, the lack of isostatic compensation and density gradients, particularly in regions where lithospheric thickness gradients are large, gives rise to lateral gradients in stress, which the real asthenosphere cannot support.

4.4 Lateral and vertical variations in the strength of the lithosphere

The end result of assuming full vertical decoupling between deeper layers of the lithosphere by decreasing the model base depth to shallow lithospheric depths is to concentrate integrated stress differences related to topography into thinner lithospheric columns, thereby increasing the magnitude of the stress as noted in previous studies that vary the model base depth (Molnar *et al.* 1993; Klein

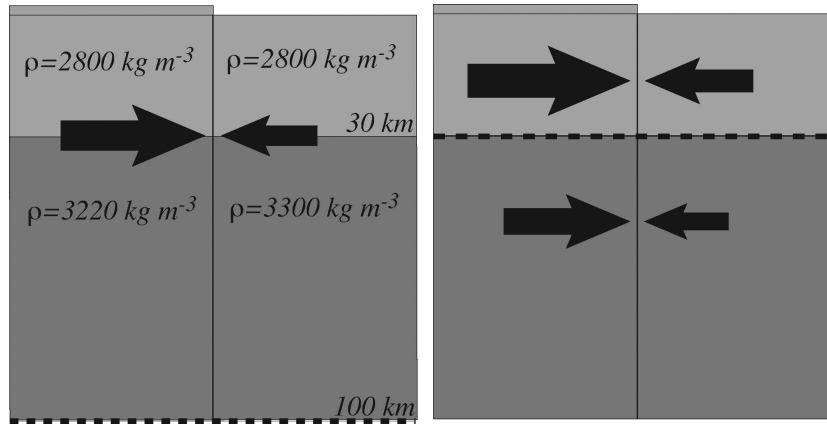


Figure 10. Density structure of two simplified lithospheric columns (left-hand side). The Moho depth and crustal density are constant, while a 2 km elevation difference exists between the two columns. The mantle density in the topographically lower column (reference column) is 3300 kg m^{-3} and the mantle density of the topographically high column is adjusted to enforce isostatic compensation at 100 km depth. The arrows represent the total mean lithostatic stress of each column, when the base depth is placed at the compensation depth. Moving the base depth to the Moho (right-hand side) implies a horizontal stress gradient with depth, as the mean lithostatic stress differences between the two columns varies above and below the base depth.

et al. 2009) or look at the depth-dependence of the stress with time (e.g. Kuszniir & Bott 1977; Bott & Kuszniir 1979; Liu *et al.* 2000). In Klein *et al.* (2009) the model is uncompensated and therefore unaccounted for basal tractions exist at the model base. As a result, the tectonic stresses calculated for a shallow model base depth are only reasonable estimates under the following conditions: horizontal stress gradients (σ_{xx} , σ_{yy}) gradients across the model base depth are small; a rheologically weak layer at the model base leads to sharp stress gradients and weak coupling between layers above and below the base depth. The validity of isolating stress fields from different sections of an isostatically balanced column depends on the lithospheric rheological structure or the distribution of stress gradients as a function of depth.

As an example, consider the stress state between two isostatically balanced lithospheric columns extending to a depth of 100 km and containing a 2 km elevation difference (Fig. 10). The crustal density and Moho depth are equal in both columns, while the mantle density in the topographically high column is adjusted to enforce isostatic compensation relative to the mantle density of 3300 kg m^{-3} in the reference column. The difference in mean lithostatic stress between the topographically high column (Ω_{top}) and reference column (Ω_{ref}) serves as a proxy for the magnitude of extension in the topographically high column. Placing the model base depth at the isostatic compensation depth generates $\sim 36 \text{ MPa}$ of extension in the topographically high column (Fig. 11). Moving the base depth above isostatic compensation depth implies two distinct horizontal tectonic stress states exist above the base depth and between the base depth and isostatic compensation depth (Fig. 10). Systematically decreasing the base depth increases the magnitude of extension in both column layers, with the stress difference across the layers ranging between $\sim 36 \text{ MPa}$ and 26 MPa (Fig. 11).

Although vertical gradients in the horizontal stress are likely much larger than those in the lithosphere due to the simplifications in this example, the results clearly demonstrate why placing the base depth at uncompensated shallow depths requires significant assumptions about the rheological structure of the lithosphere. In the case of the Western US, Klein *et al.* (2009) argued that a shallow compensation (20 km) was reasonable based on the magnitude of shear stresses related to mantle flow in the region. This analysis, however, excludes vertical gradients of horizontal stress across the shallow model base depth that result from stress gradients be-

tween the model base depth and the base of the lithosphere. If these gradients are large, then the calculated stress state in the shallow lithosphere may not be accurate unless a very weak decoupling layer exists at the base of the seismogenic lithosphere. Convection models show strong flow across regions of varying lithospheric thickness, which imply the presence of such strong gradients (Conrad & Lithgow-Bertelloni 2006). The relative strength contrast across the base depth will determine the validity of the uncompensated shallow base depth approximation. It is therefore preferable to use either expanded thin-viscous sheet approximations (Bird 1989; Medvedev & Podladchikov 1999) or full 3-D models that account for the rheological coupling between different lithospheric layers and variations in lithospheric structure.

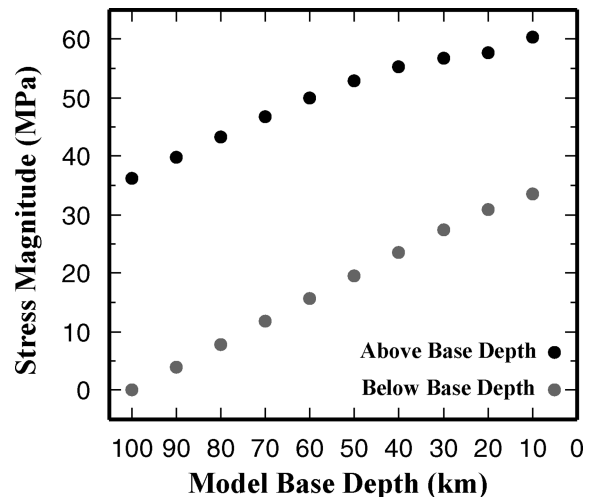


Figure 11. State of stress in the topographically high column illustrated in Fig. 10. The state of stress is defined as the difference in mean lithostatic stress between the topographically high and reference column. When the model base depth is placed above the compensation depth, distinct states of horizontal stress state exist above the base depth and between the base depth and isostatic compensation depth. The state of stress in any part of the topographically high column is extensional regardless of where the model base depth is placed.

5 CONCLUSIONS

Our results show that variations in lateral variations in mantle lithospheric density and thickness contribute significantly to the stress field. For the first time, we examined the role of realistic mantle lithosphere that contains both depleted and undepleted layers in keeping with petrological and dynamical constraints on the formation of oceanic and continental lithosphere. In this sense, a model like TDL represents a significant advance on previous studies that choose a homogenous mantle density equivalent to peridotite (3300 kg m^{-3}) or adjust it to enforce isostasy. Models like TDL are also superior because isostasy must be violated to the extent that dynamic topography is important. The density variations required to enforce isostasy must vary by as much as 3.5 per cent (6 per cent peak to peak) over a few hundred kilometres as shown in Fig. 2. These density variations are equivalent to lateral temperature variations of 1200° , in violation of observed heat flow changes over such length scales or to compositional changes from harzburgite to eclogite. Densification to eclogitic levels is not dynamically sustainable as the dense lithospheric material would eventually sink into the mantle.

We have also shown that it is the tectonic stress that balances lateral variations in Ω , which in regions of high topography or large lithospheric thickness will be larger in magnitude than the deviatoric stress. Hence, thin viscous sheets formulations are unlikely to capture the absolute magnitude of stresses needed to balance variations in lithospheric structure.

The stresses required to balance spatial gradients in Ω however, depend critically on the theoretical formulation chosen. Although representing topography, thickness and density variations by a mean lithostatic stress, as in much previous work, provides a simple and elegant procedure for studying the lithosphere, it is limited by the need for a uniform base depth and homogeneous strength. Our results show that there is a large variability in calculated tectonic stress patterns and especially magnitudes, depending on the choice of L . For the commonly assumed 100 km base depth the density structure of the mantle lithosphere has a minor impact on global tectonic stress magnitudes and orientations, which are similar to the azimuths and regimes of the World Stress Map. Increasing or decreasing L to account for deep continental roots, thin lithosphere or sharp variations in lithospheric strength strongly modifies global and regional tectonic stress patterns as the relative contributions of topography and mantle density structure change. Choosing L to be much greater than 100 km, as required to capture deep mantle lithospheric structure, produces large-scale stress patterns that no longer match the World Stress Map. Choosing L to be much shallower than 100 km, as required to exclude weak asthenosphere from the computation of Ω , also leads to worse agreement with observations. We may interpret the closer agreement for 100 km base depth as indication that this historically accepted value also represents an adequate average for lithospheric thickness (Cooper & Conrad 2009; Naliboff *et al.* 2009) and depth of compensation. However, variations in the stress field with L highlight the importance of properly accounting for the dynamic contributions to topography at depths greater than 100 km and perhaps crucially, the inherent limitations of the Ω formulation to account for variations in lithospheric thickness and depth-dependent rheology.

Modelling a specific region with relatively uniform lithospheric structure partly removes the complications of lateral variations in lithospheric thickness and density. But, regionalizing the source of stress exerts a first-order control on the regional tectonic stress patterns as shown in Figs 7 and 9. Hence, studies of the stress field

should be global and not restricted to regions like Western North America or individual plates or at the very least lateral boundary conditions should come from a global model.

The thickness and composition of the deep lithosphere, dynamic versus isostatic support of topography and the role of lateral and vertical variations in rheology in modifying tectonic stress emerge as the largest unresolved issues in our understanding of the lithospheric stress field. Of these issues, the role of density structure and lithospheric rheology are the most important in the context of the approximations most widely used in the literature and explored here as shown by our results. First-order variations in lithospheric strength (i.e. weak lower crust or the strength contrast across the Moho) lead to stress and deformation patterns that strongly depend on depth and are not captured by a single depth-averaged quantity.

Examining the depth-dependence of the stress field is particularly important in determining the relative contributions of mantle flow (basal shear), plate boundary forces, topography and lithospheric thickness and density to the stress field on a global (Steinberger *et al.* 2001; Lithgow-Bertelloni & Gynn 2004; Ghosh *et al.* 2008), plate (Humphreys & Coblenz 2007) or regional (Flesch *et al.* 2007) scale. Variations in lithospheric strength are likely to reduce the tectonic stresses related to basal shear (Steinberger *et al.* 2001), which are strongly affected by rheological boundaries. Coupling between the mantle lithosphere and upper crust may also be significantly restricted in the presence of weak layers (Pysklywec *et al.* 2002; Beaumont *et al.* 2004). This likely dependence on depth of the stress field related to the rheological structure of the lithosphere may also imply that most of the observations on the world stress map are not representative of the state of stress of lithospheric plates, but only of the shallow crust.

The future, however, is bright because of more extensive and more detailed *in situ* pictures of lithospheric structure from seismology. Large-scale deployments such as USArray and observational networks such as NIRIES and EPOS enabled by Observatories and Research Facilities for European Seismology (ORFEUS) are already producing substantial advances in our knowledge of the continental lithosphere. Ever more sophisticated experimental measurements and field studies of the rheology of the lithosphere and mantle (e.g. Homburg *et al.* 2010) combined with global and regional determinations of elastic thickness across tectonic provinces (Bechtel *et al.* 1990; Lowry & Smith 1995; Lowry *et al.* 2000; Burov 2010 and references therein) will provide a more complete picture of vertical and lateral changes in lithospheric strength. Coupled with state-of-the-art thermodynamic methods for determining relevant physical properties as a function of composition, temperature and pressure (Stixrude & Lithgow-Bertelloni 2011) we are not far from having the information necessary to study the effects of 3-D variations in density and rheology on Earth's surface deformation.

Future studies of the lithospheric stress field must begin to take advantage of such developments by solving in 3-D the equations of mechanical equilibrium and including vertical and lateral variations in rheological properties to capture fully the effects of varying density and thickness in the mantle lithosphere and the extent of mechanical coupling between shallow and deep lithospheric regions, as well as the mantle.

ACKNOWLEDGMENTS

We thank Greg Houseman, an anonymous reviewer and Stephane Labrosse for comments that greatly improved the manuscript. All figures were prepared using GMT version 4.2.0 by P. Wessel and

W. F. Smith. This work was supported by NSF grant and EAR-0609553 (CL-B).

REFERENCES

- ABAQUS/Standard, 2010. *Abaqus Theory and Analysis Manual Version 6.10*, Dassault Systèmes, Providence, RI, USA.
- Artemieva, I.M., 2006. Global 1 degrees x 1 degrees thermal model TC1 for the continental lithosphere: Implications for lithosphere secular evolution, *Tectonophysics*, **416**, 245–277.
- Artemieva, I.M. & Mooney, W.D., 2001. Thermal thickness and evolution of Precambrian lithosphere: a global study, *J. geophys. Res.*, **106**(B8), 16 837–16 414, doi:10.1029/2000JB900439.
- Artyushkov, E.V., 1973. Stresses in the lithosphere caused by crustal thickness inhomogeneities, *J. geophys. Res.*, **78**(32), 7675–7708, doi:10.1029/JB078i032p07675.
- Asimow, P.D., Hirschmann, M.M., Ghiorso, M.S., O'Hara, M.J. & Stolper, E.M., 1995. The effect of pressure-induced solid-solid phase-transitions on decompression melting of the mantle, *Geochim. Cosmochim. Acta*, **59**(21), 4489–4506.
- Bassin, C., Laske, G. & Masters, G., 2000. The current limits of resolution for surface wave tomography in North America, *EOS, Trans. Am. geophys. Un.*, **81**(48), Fall Meeting Suppl., Abstract S12A-03.
- Beaumont, C., Jamieson, R.A., Nguyen, M.H. & Medvedev, S., 2004. Crustal channel flows: 1. Numerical models with applications to the tectonics of the Himalayan-Tibetan orogen, *J. geophys. Res.*, **109**, B06406, doi:10.1029/2003JB002809.
- Bechtel, T.D., Forsyth, D.W., Sharpotn, V.L. & Grieve, R.A.F., 1990. Variations in effective elastic thickness of the North American lithosphere, *Nature*, **343**, 636–638.
- Bird, P., 1989. New finite element techniques for modeling deformation histories of continents with stratified temperature-dependent rheology, *J. geophys. Res.*, **94**(B4), 3967–3990.
- Bott, M.H.P. & Kusznir, N.J., 1979. Stress distributions associated with compensated plateau uplift structures with application to the continental splitting mechanism, *Geophys. J. R. astr. Soc.*, **56**, 451–459.
- Burgmann, R. & Dresen, G., 2008. Rheology of the lower crust and upper mantle: evidence from rock mechanics, geodesy and field observations, *Annu. Rev. Earth planet. Sci.*, **36**, 531–567.
- Burov, E.B., 2010. The equivalent elastic thickness ($T(e)$), seismicity and the long-term rheology of continental lithosphere: Time to burn-out “creme brulee”? Insights from large-scale geodynamic modeling, *Tectonophysics*, **484**(1–4), 4–26.
- Burov, E.B. & Watts, A.B., 2006. The long-term strength of continental lithosphere: “jelly sandwich” or “creme brulee”? *GSA Today*, **16**(1), 4–10.
- Clark, M. K. & Royden, L.H., 2000. Topographic ooze: building the eastern margin of Tibet by lower crustal flow, *Geology*, **28**, 703–706.
- Coblentz, D.D., Richardson, R.M. & Sandiford, M., 1994. On the gravitational potential of the Earth's lithosphere, *Tectonics*, **13**(4), 929–945.
- Conrad, C.P. & Lithgow-Bertelloni, C., 2006. Influence of continental roots and asthenosphere on plate-mantle coupling, *Geophys. Res. Lett.*, **33**, L05312, doi:10.1029/2005GL025621.
- Conrad, C.P., Lithgow-Bertelloni, C. & Loudon, K.E. 2004. Iceland, the Farallon slab, and dynamic topography of the North Atlantic, *Geology*, **32**, 177–180.
- Cooper, C.M. & Conrad, C.P., 2009. Does the mantle control the maximum thickness of cratons? *Lithosphere*, **1**(2), 67–72.
- Dahlen, F.A., 1981. Isostasy and the ambient state of stress in the oceanic lithosphere, *J. geophys. Res.*, **86**, 7801–7807.
- De Koker, N.P., Lithgow-Bertelloni, C. & Stixrude, L., 2005. Dynamic topography and the density structure of the mantle lithosphere, *EOS, Trans. Am. geophys. Un.*, **86**(52), Fall Meet. Suppl., Abstract T23A-0524.
- England, P. & Houseman, G., 1986. Finite strain calculations of continental deformation 2. Comparison with the India-Asia collision zone, *J. geophys. Res.*, **91**(B3), 3664–3676.
- England, P. & Houseman, G., 1988. The mechanics of the Tibetan plateau, *Phil. Trans. R. Soc. Lond.*, **326**(1589), 301–319.
- England, P. & Houseman, G., 1989. Extension during continental convergence, with application to the Tibetan Plateau, *J. geophys. Res.*, **94**(B12), 17 561–17 579.
- England, P. & McKenzie, D., 1982. A thin viscous sheet model for continental deformation, *Geophys. J. R. astr. Soc.*, **70**(2), 295–321.
- England, P. & McKenzie, D., 1983. Correction to: a thin viscous sheet model for continental deformation, *Geophys. J. R. astr. Soc.*, **73**, 523–532.
- England, P. & Molnar, P., 1997. Active deformation of Asia: from kinematics to dynamics, *Science*, **278**, 647–650.
- Fleitout, L. & Froidevaux, C., 1982. Tectonics and topography for a lithosphere containing density heterogeneities, *Tectonics*, **1**(1), 21–56.
- Fleitout, L. & Froidevaux, C., 1983. Tectonic stresses in the lithosphere, *Tectonics*, **2**(3), 315–324.
- Flesch, L.M., Holt, W.E., Haines, A.J. & Shen-Tu, B., 2000. Dynamics of the Pacific-North American plate boundary in the western United States, *Science*, **287**, 834–836.
- Flesch, L.M., Haines, A.J. & Holt, W.E., 2001. Dynamics of the India-Eurasia collision zone, *J. geophys. Res.*, **106**(B8), 16 435–16 460.
- Flesch, L.M., Holt, W.E., Haines, A.J., Wen, L.X. & Shen-Tu, B., 2007. The dynamics of western North America: stress magnitudes and the relative role of gravitational potential energy, plate interaction at the boundary and basal tractions, *Geophys. J. Int.*, **169**, 866–896.
- Ghosh, A., Holt, W.E., Flesch, L.M. & Haines, A.J., 2006. Gravitational potential energy of the Tibetan Plateau and the forces driving the Indian plate, *Geology*, **34**(5), 321–324.
- Ghosh, A., Holt, W.E., Wen, L., Haines, A.J. & Flesch, L.M., 2008. Joint modeling of lithosphere and mantle dynamics elucidating lithosphere-mantle coupling, *Geophys. Res. Lett.*, **35**(L16309), doi:10.1029/2008GL034365.
- Ghosh, A., Holt, W.E., Flesch, L.M. & Haines, A.J., 2009. Contribution of gravitational potential energy differences to the global stress field, *Geophys. J. Int.*, **179**, 787–812.
- Gung, Y.C., Panning, M. & Romanowicz, B., 2003. Global anisotropy and the thickness of continents, *Nature*, **422**, 707–711.
- Hager, B.H., Clayton, R.W., Richards, M.A., Comer, R.P. & Dziewonski, A.M., 1985. Lower mantle heterogeneity, dynamic topography and the geoid, *Nature*, **313**, 541–545.
- Hartz, E.H. & Podladchikov, Y.Y., 2008. Toasting the jelly sandwich: the effect of shear heating on lithospheric geotherms and strength, *Geology*, **36**(4), 331–334.
- Homburg, J.M., Hirth, G. & Kelemen, P. B., 2010. Investigation of the strength contrast at the Moho: a case study from the Oman Ophiolite, *Geology*, **38**(8), 679–682.
- Houseman, G. & England, P., 1993. Crustal thickening versus lateral expulsion in the Indian-Asian Continental Collision, *J. geophys. Res.*, **98**(B7), 12 233–12 249.
- Humphreys, E.D. & Coblenz, D.D., 2007. North American dynamics and Western US Tectonics, *Rev. Geophys.*, **45**, RG3001, doi:10.1029/2005RG000181.
- Jackson, J., 2002. Strength of the continental lithosphere: time to abandon the jelly sandwich?, *GSA Today*, **12**(9), 4–10.
- Jaupart, C. & Mareschal, J.C., 1999. The thermal structure and thickness of continental roots, *Lithos*, **48**, 93–114.
- Jeffreys, H., 1984. *Cartesian Tensors*, 7th edn, Cambridge University Press, Cambridge, 98pp.
- Jones, C.H., Unruh, J.R. & Sonder, L.J., 1996. The role of gravitational potential energy in active deformation in the southwestern United States, *Nature*, **381**, 37–41.
- Jones, C.H., Sonder, L.J. & Unruh, J.R., 1998. Lithospheric gravitational potential energy and past orogenesis: implications for conditions of initial Basin and Range and Laramide deformations, *Geology*, **26**(7), 639–642.
- Jordan, T.H., 1975. The continental tectosphere, *Rev. Geophys.*, **13**(3), 1–12.
- Kaban, M.K., Schwintzer, P., Artemieva, M. & Mooney, W.D., 2003. Density of the continental roots: compositional and thermal contributions, *Earth planet. Sci. Lett.*, **209**(1–2), 53–69.

- Klein, E. & Langmuir, C., 1987. Global correlations of ocean ridge basalt chemistry with axial depth and crustal thickness, *J. geophys. Res.*, **92**(B8), 8089–8115.
- Klein, E.C., Flesch, L.M., Holt, W.E. & Haines, A.J., 2009. Evidence of long-term weakness on seismogenic faults in western North America from dynamic modeling, *J. geophys. Res.*, **114**, B03402, doi:10.1029/2007JB005201.
- Kohlstedt, D.L., Evans, B. & Mackwell, D.J., 1995. Strength of the lithosphere – constraints imposed by laboratory experiments, *J. geophys. Res.*, **100**(B9), 17 587–17 602.
- Kusznir, N.J. & Bott, M.H.P., 1977. Stress concentrations in the upper lithosphere caused by underlying visco-elastic creep, *Tectonophysics*, **43**, 247–256.
- Levander, A., Niu, F. & Miller, M.S., 2008. The Moho and the Lithosphere-Asthenosphere Boundary under the western U.S. from USArray PdS Receiver Functions, *EOS, Trans. Am. geophys. Un.*, **89**(53), Fall Meet. Suppl., Abstract S31D-05.
- Li, X., Yuan, X. & Kind, R., 2007. The lithosphere-asthenosphere boundary beneath the western United States, *Geophys. J. Int.*, **170**(2), 700–710.
- Lithgow-Bertelloni, C. & Guynn, J.H., 2004. Origin of the lithospheric stress field, *J. geophys. Res.*, **109**, B01408, doi:10.1029/2003JB002467.
- Lithgow-Bertelloni, C. & Silver, P.G., 1998. Dynamic topography, plate driving forces and the African superswell, *Nature*, **395**, 269–272.
- Liu, M. & Yang, Y., 2003. Extensional collapse of the Tibetan Plateau: Results of three-dimensional finite element modeling, *J. geophys. Res.*, **108**(B8), 2361, doi:10.1029/2002JB002248.
- Liu, M., Shen, Y. & Yang, Y., 2000. Gravitational collapse of orogenic crust: a preliminary three-dimensional finite element study, *J. geophys. Res.*, **105**(B2), 3159–3173.
- Lowry, A.R. & Smith, R.B., 1995. Strength and rheology of the western U.S. Cordillera, *J. geophys. Res.*, **100**(B9), 17 947–17 963.
- Lowry, A.R., Ribe, N.M. & Smith, R.B., 2000. Dynamic elevation of the Cordillera, western United States, *J. geophys. Res.*, **105**(B10), 23 371–23 390.
- Mancktelow, N.S., 2008. Tectonic pressure: theoretical concepts and modelled examples, *Lithos*, **103**, 149–177.
- Masters, G. & Gubbins, D., 2003. On the resolution of density within the earth, *Phys. Earth planet. Inter.*, **140**, 159–167.
- Medvedev, S.E. & Podladchikov, Y., 1999. New extended thin-sheet approximation for geodynamic applications—I. Model formulation, *Geophys. J. Int.*, **136**, 567–585.
- Michaut, C. & Jaupart, C., 2004. Nonequilibrium temperatures and cooling rates in thick continental lithosphere, *Geophys. Res. Lett.*, **31**, L24602, doi:10.1029/2004GL021092.
- Molnar, P. & Lyon-Caen, H., 1988. Some simple physical aspects of the support, structure, and evolution of mountain belts, *Geol. Soc. Am., Spec. Paper.*, **218**, 179–207.
- Molnar, P. & Tapponnier, P., 1978. Active tectonics of Tibet, *J. geophys. Res.*, **83**(B11), 5361–5376.
- Molnar, P., England, P. & Martinod, J., 1993. Mantle dynamics, uplift of the Tibetan Plateau, and the Indian Monsoon, *Rev. Geophys.*, **31**(4), 357–396.
- Muller, R.D., Roest, W.R., Royer, J.-Y., Gahagan, L.M. & Sclater, J.G., 1997. Digital isochrons of the world's ocean floor, *J. geophys. Res.*, **102**(B2), 3211–3214.
- Naliboff, J.B., 2010. Dependence of the stress field on plate-mantle coupling and lithospheric structure, *PhD thesis*, Univ. Michigan, Ann Arbor, MI.
- Naliboff, J.B., Conrad, C. P. & Lithgow-Bertelloni, C., 2009. Modification of the lithospheric stress field by lateral variations in plate-mantle coupling, *Geophys. Res. Lett.*, **36**, L22307, doi:10.1029/2009GL040484.
- Pascal, C., 2006. On the role of heat flow, lithosphere thickness and lithosphere density on gravitational potential stresses, *Tectonophysics*, **425**(1–4), 83–99.
- Pollack, H. & Chapman, D., 1977. On the regional variation of heat flow, geotherms, and lithospheric thickness, *Tectonophysics*, **38**, 279–296.
- Pysklywec, R.N., Beaumont, C. & Fullsack, P., 2002. Lithospheric deformation during the early stages of continental collision: numerical experiments and comparison with South Island, New Zealand, *J. geophys. Res.*, **107**(B7), 2133, doi:10.1029/2001JB000252.
- Regenauer-Lieb, K., Weinberg, R.F. & Rosenbaum, G., 2006. The effect of energy feedbacks on continental strength, *Nature*, **442**, 67–70.
- Richardson, R.M., 1992. Ridge forces, absolute plate motions, and the intraplate stress field, *J. geophys. Res.*, **97**(B8), 11 739–11 748.
- Richardson, R.M. & Redding, L.M., 1991. North-American plate dynamics, *J. geophys. Res.*, **96**(B7), 12 201–12 223.
- Richardson, R.M., Solomon, S.C. & Sleep, N.H., 1978. Tectonic stress in the plates, *Rev. Geophys.*, **17**(5), 981–1019.
- Royden, L.H., Burchfiel, B., King, R.W., Wang, E., Chen, Z., Shen, F. & Liu, Y., 1997. Surface deformation and lower crustal flow in Eastern Tibet, *Science*, **276**, 788–790.
- Rudnick, R.L., McDonough, W.F. & O'Connell, R.J., 1998. Thermal structure, thickness and composition of continental lithosphere, *Chem. Geol.*, **145**(3–4), 395–411.
- Steinberger, B., Schmeling, H. & Marquart, G., 2001. Large-scale lithospheric stress field and topography induced by global mantle circulation, *Earth planet. Sci. Lett.*, **186**(1), 75–91.
- Stixrude, L. & Lithgow-Bertelloni, C., 2005. Thermodynamics of mantle minerals – I. Physical properties, *Geophys. J. Int.*, **162**(2), 610–632.
- Stixrude, L. & Lithgow-Bertelloni, C., 2011. Thermodynamics of mantle minerals – II. Phase equilibria, *Geophys. J. Int.*, **184**(3), 1180–1213.
- Thatcher, W. & Pollitz, F.F., 2008. Temporal evolution of continental lithospheric strength in actively deforming regions, *GSA Today*, **18**(4/5), 4–11, doi:10.1130/GSAT01804-5A.1.
- Turcotte, D.L., 1983. Mechanisms of crustal deformation, *J. Geol. Soc.*, **140**(5), 701–724.
- Workman, R.K. & Hart, S.R., 2005. Major and trace element composition of the depleted MORB mantle (DMM), *Earth planet. Sci. Lett.*, **231**, 53–72.
- Xu, X., Lithgow-Bertelloni, C. & Conrad, C.P., 2006. Reconstructions of Cenozoic seafloor ages: implications for sea level, *Earth planet. Sci. Lett.*, **243**, 552–564.
- Yuan, H., & Romanowicz, B., 2010. Lithospheric layering in the North American Craton, *Nature*, **466**, 1063–1068.
- Zandt, G., Myers, S.C. & Wallace, T.C., 1995. Crust and mantle structure across the Basin and Range-Colorado Plateau boundary at 37°N latitude and implications for Cenozoic extensional mechanism, *J. geophys. Res.*, **100**(B6), 10 529–10 548.
- Zoback, M.L., 1992. First- and second-order patterns of stress in the lithosphere: the world stress map project, *J. geophys. Res.*, **97**(B8), 11 703–11 728.
- Zoback, M.L. & Mooney, W.D., 2003. Lithospheric buoyancy and continental intraplate stresses, *Int. Geol. Rev.*, **45**, 95–118.

APPENDIX A

A1 Stress and pressure

The lithosphere behaves like a solid on timescales that are short compared with its Maxwell relaxation time τ_M . Because τ_M approaches or exceeds geologic timescales, the lithosphere is capable of supporting deviatoric stresses. This means that the stress tensor is not isotropic, as it would be in a pure fluid, and the diagonal components are not all equal to the pressure. In a solid, the relationship between the stress tensor σ_{ij} and pressure p (a scalar quantity), is therefore non-trivial and is given by the relationship

$$p = -\frac{1}{3}\sigma_{kk}. \quad (\text{A1})$$

In this equation and throughout we assume the Einstein summation convention (Jeffreys 1984), so that pressure is defined as negative one-third the trace of the stress tensor. The negative sign originates in the historical convention that pressure be positive on compression, whereas stress is positive on tension. The sign convention for stress agrees with the convention that strain be positive on extension and leads to the usual definition of the elastic constants as being positive for mechanically stable solids.

In the lithosphere, the pressure is not simply related to the lithostatic stress due the weight of the overlying column of rock. Rather, it is the spatial gradients in the vertical component of the stress tensor (σ_{zz}) and the shear stresses (σ_{xz} , σ_{yz}) acting on the vertical face that balance the weight of the overburden as required by the equation of mechanical equilibrium

$$\frac{\partial \sigma_{ij}}{\partial x_j} = -\rho g_i. \quad (\text{A2})$$

However, at the length-scales of interest and in keeping with much prior literature we may consider the shear stresses on the vertical face ($\sigma_{xz} = \sigma_{yz} = 0$) to be negligible so that eq. (A2) reads for $i = z$, where z is positive upwards

$$\frac{\partial \sigma_{zz}}{\partial z} = \rho g, \quad (\text{A3})$$

where ρ is the density and g_i is the gravitational acceleration vector with components $(0, 0, -g)$. The remaining components of the stress tensor are related to tectonic forces that drive deformation. The contribution from these non-lithostatic components is highlighted in the tectonic stress, which we define as

$$\sigma_{ij}^T = \sigma_{ij} - \sigma_{zz} \delta_{ij}, \quad (\text{A4})$$

where δ_{ij} is the Kronecker delta tensor. We consider the tectonic stress defined in this way to be a more complete measure of the forces that control the response of the lithosphere to the lateral variations in structure that arise in the course of geological history. In general, the tectonic stress tensor is not identical to the deviatoric stress tensor that arises naturally in the development of fluid dynamics as the difference between the stress and the pressure

$$\tau_{ij} = \sigma_{ij} + p \delta_{ij} \quad (\text{A5})$$

Substituting eq. (A5) into eq. (A4) gives

$$\sigma_{ij}^T = \tau_{ij} - \tau_{zz} \delta_{ij} \quad (\text{A6})$$

through the relationship between the lithostatic stress and the pressure $\tau_{zz} = \sigma_{zz} + p$, which vanishes for an isotropic stress state, such as one may find in a stationary fluid. The tectonic stress tensor is a generalization of Mancktelow's (2008) tectonic pressure.

A2 Origin of tectonic stress

Lateral variations in density and layer thickness cannot be supported in a stationary fluid. In a solid, such as the lithosphere, these lateral variations are balanced by tectonic stresses. We derive this relationship, starting from the equation of mechanical equilibrium (eq. A2). To maintain contact with previous work (England & McKenzie 1982, 1983), we derive the equations in terms of deviatoric stress, and recast the final result in terms of tectonic stress.

Lithospheric structure varies laterally on scales ranging from the width of a fault zone to that of continents. We focus here on lateral variations in lithospheric loading on scales longer than the thickness of the lithosphere, so that the shear stresses on the vertical face ($\sigma_{xz} = \tau_{xz}$, $\sigma_{yz} = \tau_{yz}$, by the definition of deviatoric stress) as previously stated are negligible (Artyushkov 1973)

$$\tau_{xz} = \tau_{yz} = 0. \quad (\text{A7})$$

Substituting eq. (A5) into eq. (A2) we obtain

$$\frac{\partial \tau_{ij}}{\partial x_j} = \frac{\partial p}{\partial x_i} i, \quad j = x, y \quad (\text{A8})$$

$$\frac{\partial \tau_{zz}}{\partial z} - \frac{\partial p}{\partial z} = \rho g. \quad (\text{A9})$$

Eq. (A8) is identical to eq. 13 of England & McKenzie (1983). The appearance of the pressure in these equations derives directly from the definition of pressure in terms of the stress (eq. A1) and makes no assumptions about the isotropy of the state of stress.

We assume that the surfaces of the lithosphere are traction free so that the weight of the lithosphere is balanced by the stress gradient and the deviatoric stresses can be averaged with depth (eq. A9)

$$\frac{\partial \tau_{ij}}{\partial z} = 0. \quad (\text{A10})$$

It is convenient to work with the depth-integrated form of eq. (A8).

$$\frac{1}{L+h} \int_0^{L+h} \frac{\partial \tau_{ij}(z')}{\partial x_j} dz' = \frac{1}{L+h} \int_0^{L+h} \frac{\partial p(z')}{\partial x_i} dz' \quad (\text{A11})$$

and to define the depth-averaged quantities

$$\bar{\tau}_{ij} = \frac{1}{L+h} \int_0^{L+h} \tau_{ij}(z') dz' = \tau_{ij} \quad (\text{A12})$$

$$\bar{p} = \frac{1}{L+h} \int_0^{L+h} p(z') dz', \quad (\text{A13})$$

where we choose our coordinate system such that z is positive upwards, $z = 0$ is the base of the lithosphere and $z = L + h$ is the free surface, L is the uniform lithospheric thickness and h is the topography. The second equality in eq. (A12) follows from the depth-independence of the deviatoric stresses (eq. A10).

Examining the quantity

$$\frac{\partial \bar{p}}{\partial x_i} = -\frac{1}{(L+h)^2} \frac{\partial h}{\partial x_i} \int_0^{L+h} p(z') dz' + \frac{1}{(L+h)} \frac{\partial}{\partial x_i} \int_0^{L+h} p(z') dz' \quad (\text{A14})$$

the second term on the right hand side must be evaluated using Leibniz's rule and

$$\begin{aligned} \frac{\partial \bar{p}}{\partial x_i} = & -\frac{1}{(L+h)^2} \frac{\partial h}{\partial x_i} \int_0^{L+h} p(z') dz' \\ & + \frac{1}{(L+h)} \left[\int_0^{L+h} \frac{\partial p(z')}{\partial x_i} dz' + p(L+h) \frac{\partial h}{\partial x_i} \right], \end{aligned} \quad (\text{A15})$$

evaluating pressure terms we find the first term is related to \bar{p} and the other two vanish

$$\frac{\partial \bar{p}}{\partial x_i} = -\frac{\bar{p}}{(L+h)} \frac{\partial h}{\partial x_i} + \frac{1}{(L+h)} \int_0^{L+h} \frac{\partial p(z')}{\partial x_i} dz', \quad (\text{A16})$$

rearranging and substituting into eq. (A11) we find

$$\frac{\partial \bar{\tau}_{ij}}{\partial x_j} = \frac{\partial \bar{p}}{\partial x_i} + \frac{\bar{p}}{(L+h)} \frac{\partial h}{\partial x_i}. \quad (\text{A17})$$

England & McKenzie (1982) and subsequent authors have assumed that the second term is negligible.

We can relate \bar{p} to the density structure of the lithosphere. Integrating the vertical component (eq. A3) of the equations of mechanical equilibrium:

$$\sigma_{zz}(z) = \tau_{zz}(z) - p(z) = g \int_0^z \rho(z') dz' + f(x, y), \quad (\text{A18})$$

where $f(x, y)$ is the most general form possible of the integration constant. The boundary conditions are $\sigma_{zz} = -P_0$ at $z = 0$ and $\sigma_{zz} = 0$ at $z = L+h$. Then

$$f(x, y) = -P_0 = -g \int_0^{L+h} \rho(z') dz'. \quad (\text{A19})$$

In eq. (12) of England & McKenzie (1983) the last equality $f(x, y) = -\rho_m Lg$, where ρ_m is the mantle density, relies on the additional assumption of isostasy. Substituting and rearranging

$$p(z) = \tau_{zz}(z) - \sigma_{zz}(z) = \tau_{zz}(z) + P_0 - g \int_0^z \rho(z') dz', \quad (\text{A20})$$

where the second equality follows from eq. (A19). The depth-averaged pressure is

$$\bar{p} = \bar{\tau}_{zz} + P_0 - \frac{g}{L+h} \int_0^{L+h} dz' \int_0^{z'} \rho(z'') dz'' = \bar{\tau}_{zz} - \Omega, \quad (\text{A21})$$

where the last equality defines Ω , the mean lithostatic stress

$$\Omega = \bar{\sigma}_{zz}. \quad (\text{A22})$$

The presence of P_0 in Ω does not matter for the resulting stresses since it is a constant. When computing lithospheric stresses only the differences in Ω between adjacent columns of lithosphere matter, because there are no lateral variations in P_0 for isostatically compensated lithosphere. The precise value of that integration constant depends on the definition of the coordinate system (whether z is 0 at the base of the lithosphere or as we assumed, at its surface). For example, if z were defined positive downward, and $z = 0$ at the free surface where P must be 0, $f(x, y)$ in eq. (A19) would be 0.

Substituting eq. (A21) into eq. (A17) yields

$$\frac{\partial}{\partial x_j} (\bar{\tau}_{ij} + \bar{\tau}_{ii} \delta_{ij}) + \frac{\partial \Omega}{\partial x_i} = \frac{(-\bar{\tau}_{ii} - \Omega)}{(L+h)} \frac{\partial h}{\partial x_i} i, \quad j = x, y, \quad (\text{A23})$$

where we have used the definition of deviatoric stress $\bar{\tau}_{zz} = -\bar{\tau}_{xx} - \bar{\tau}_{yy} = -\bar{\tau}_{ii} i = x, y$. The left hand side is the integrand in eq. 9 of Ghosh *et al.* (2009), who follow England & McKenzie (1982) in assuming that topographic slopes are sufficiently gentle that the term involving $\partial h / \partial x_i$ on the right hand side is vanishingly small. The latter, however, may not be true in a mountain range.

To now recast eq. (A23) in terms of the tectonic stress (eq. A6) it is easiest to explicitly leave the terms containing $\bar{\tau}_{zz}$ and \bar{p} when performing the substitution described above, so that we may now write

$$\frac{\partial}{\partial x_j} (\bar{\tau}_{ij} - \bar{\tau}_{zz} \delta_{ij}) = -\frac{\partial \Omega}{\partial x_i} + \frac{\bar{p}}{(L+h)} \frac{\partial h}{\partial x_i}. \quad (\text{A24})$$

The operand on the left hand side is the definition of the tectonic stress tensor from eq. (A6), which allows us to simplify eq. (A24) as

$$\frac{\partial \bar{\sigma}_{ij}^T}{\partial x_j} = -\frac{\partial \Omega}{\partial x_i} + \frac{\bar{p}}{(L+h)} \frac{\partial h}{\partial x_i}. \quad (\text{A25})$$

Eq. (A25) shows that variations in the mean lithostatic stress (Ω) are balanced by gradients in the tectonic stress tensor, independent of rheology as noted by Molnar & Lyon-Caen (1988). However, to solve eq. (A20) a constitutive law is required, in which case the rheology of the lithosphere may shift around the various components of the stress tensor in response to Ω and its geographical variation. For example, in the case of an elastic lithosphere, which is compressible, loading leads to changes in volume (isotropic strain), which must be balanced by isotropic stresses of the same order as the original loads.

We note how remarkable it is that the entire 3-D problem can be cast as a 2-D problem, as shown by England & McKenzie (1982, 1983). This results directly from the vanishing of the bending stresses, which permits the separation of the equations of mechanical equilibrium (eq. A2) into equations involving only the horizontal stresses (eq. A8), from which the final result (eq. A25) derives. Mathematically, because $\tau_{xz} = \tau_{yz} = 0$, the stress tensor becomes a block diagonal matrix, so that the normal vertical component of the stress (σ_{zz}) does not interact with the horizontal components. Therefore, principal stresses extracted from the horizontal 2×2 stress tensor will be identical to those in the horizontal plane for the 3-D stress tensor.